Skeletal impact of 17β-estradiol in T cell-deficient mice: age-dependent bone effects and osteosarcoma formation

Julia N Cheng[1], Jennifer B Frye[2], Susan A Whitman[2], Janet L Funk[2,3,*]

[1]Cancer Biology Graduate Interdisciplinary Program, University of Arizona, 1656 E. Mabel St, Medical Research Building Rm 418, Tucson, AZ 85724

[2]Department of Medicine, University of Arizona, 1656 E. Mabel St, Medical Research Building Rm 418, Tucson, AZ 85724

[3]Department of Nutritional Sciences, University of Arizona, 1656 E. Mabel St, Medical Research Building Rm 418, Tucson, AZ 85724

Abstract

Estrogen (E_2)-dependent ER+ breast cancer, the most common breast cancer subtype, is also the most likely to metastasize to bone and form osteolytic lesions. However, ER+ breast cancer bone metastasis human xenograft models in nude mice are rarely studied due to complexities associated with distinguishing possible tumoral vs bone microenvironmental effects of E_2. To address this knowledge gap, we systematically examined bone effects of E_2 in developing young (4-week-old) vs. skeletally mature (15-week-old) female *Foxn1^{nu}* nude mice supplemented with commercial 60-day slow-release E_2 pellets and doses commonly used for ER+ xenograft models. E_2 pellets (0.05 – 0.72 mg) were implanted subcutaneously and longitudinal changes in hind limb bones (vs. age-matched controls) were determined over 6 weeks by dual-energy X-ray absorptiometry (DXA), microCT, radiographic imaging, and histology, concurrent with assessment of serum levels of E_2 and bone turnover markers. All E_2 doses tested induced significant and identical increases in bone density (BMD) and volume (BV/TV) in 4-week-old mice with high bone turnover, increasing bone mineral content (BMC) while suppressing increases in bone area (BA). E_2 supplementation, which caused dose-dependent changes in circulating E_2 that were not sustained, also led to more modest increases in BMD and BV/TV in skeletally mature 15-week-old mice. Notably, E_2-supplementation induced osteolytic osteosarcomas in a subset of mice independent of age. These results demonstrate that bone effects of E_2 supplementation should be accounted for when assessing ER+ human xenograft bone metastases models.

Keywords

Estradiol; athymic nude mice; slow-release pellets; bone mineral density; osteosarcoma

---

1. Introduction

A considerable rate of mortality in women is attributable to estrogen-dependent cancers, of which breast cancer is a leading example—1 in 8 women are affected, with one third ultimately developing incurable metastatic disease [1]. The use of human xenografts in mice to model these conditions, including patient derived xenografts, provides an important avenue for optimizing therapies [2–4]. The required use of immunodeficient or immunologically humanized mice for these studies is well established [5]. Less well recognized, perhaps, are important differences in estrogen metabolism between mice and humans that may also affect the modeling of estrogen-dependent breast or other cancers in mice. Circulating 17β-estradiol (E_2) levels are, on average, 10-fold lower in female mice as compared to women [6]. Aromatase expression in mammary tissue and osteoblastic cells in bone, which contributes to breast cancer progression and alters bone metabolism in humans, is absent in mice [7,8]. Once ovariectomized (OVX), female mice, unlike humans, also lack an extragonadal source of precursors for aromatase-mediated conversion to E_2 [7]. Furthermore, T-cell deficient athymic "nude" mice commonly used for human tumor xenograft models, including breast cancer, have even lower circulating E_2 levels compared to other mice [9,10]. Thus, orthotopic nude mouse models of estrogen receptor-positive (ER+) human breast cancer, the most common breast cancer type (>70% [11]), require supplementation with supraphysiologic levels of E_2 (relative to mouse) to support mammary tumor growth [10,12–14].

Bone is a frequent site of breast cancer metastases, particularly for ER+ tumors [15,16]. The development of human xenograft models of ER+ breast cancer bone metastasis is therefore of great clinical relevance. Most human xenograft breast cancer bone metastasis models in widespread use are ER- [3]. Modulation of the estrogenic milieu in ER- bone metastasis models in nude mice by OVX and/or E_2 supplementation has provided some information regarding possible microenvironment-specific effects of E_2 relevant to metastatic progression in bone [17–23]. However, these data are sparse and lack systematic evaluation of dose-dependent estrogenic effects. Published studies investigating E_2-supplemented human xenograft models of ER+ breast cancer bone metastasis in nude mice are also few in number and have not included assessments of dose or age dependent effects of E_2 on either bone or tumors [22–30]. Indeed, bone (vs. tumoral) effects of the single E_2 doses used in these studies are only rarely noted [22,28], and pertinent details related to E_2 dosing when using commercial sustained-release E_2 pellets, which are defined by both E_2 content and duration of release, are often not stated, thus preventing experimental replication [22,24–28].

While dose- and age-dependent E_2 effects on bone for immunocompetent mice strains have been well described [31–34], a systematic analysis of similar end-points in nude mice is lacking. Because strain-specific bone phenotypes and responses to hormonal modulation are well known [35,36], including a lack of bone loss in T cell deficient nude mice following OVX [37], an evaluation of bone effects of supraphysiologic E_2 supplementation in immunodeficient nude mice is required in order to optimize experimental designs and interpret bone-related outcomes. To address this issue, we report here on dose-dependent effects of E_2 supplementation on bone when administered to developing vs. skeletally mature *Foxn1^{nu}* athymic nude mice, using commercial subcutaneously implanted E_2-

containing slow-release pellets that are in widespread use to support human tumor growth in immunocompromised mice [12–14,22–28,30].

2. Methods

2.1. E_2 supplementation of mice.

All animal protocols were approved by the Institutional Animal Care and Use Committee at The University of Arizona in accordance with the National Institutes of Health Guide for the Care and Use of Laboratory Animals. Female *Foxn1^{nu}* athymic nude outbred mice (Envigo, Indianapolis, IN) were housed in plastic cages in laminar flow isolated hoods with access to water and autoclaved mouse chow ad libitum. Sixty-day extended-release 17β-estradiol (E_2) pellets (0.05, 0.10, 0.18, 0.36, or 0.72 mg, Innovative Research of America, Sarasota, FL) were placed subcutaneously in either 4- or 15–16 week-old mice (n=3–8/group). Naïve control mice were not supplemented with E_2 pellets.

2.2. Bone Imaging.

Complementary bone imaging modalities were used to examine E_2 effects on mouse tibiae and/or femora during a 6 week period following E_2 pellet placement in either young developing (4 week) or skeletally mature (15 week) mice. Dual-energy X-ray absorptiometry (DXA) and radiographic images (Faxitron UltraFocus 1000, Faxitron Bioptics, Tucson, AZ) were obtained weekly in anesthetized mice. Microcomputed tomography (microCT) imaging of excised hind tibiae was conducted 2 or 6 weeks post-initiation of E_2 supplementation (Scanco microCT 50, Scanco Medical, Basserdorf, Switzerland) by the Endocrine Research Unit at the San Francisco Veterans Affairs Medical Center. Trabecular bone in the proximal tibial metaphysis was assessed using 100 serial cross-sectional scans (10-μm voxel size) of the secondary spongiosa, extending proximally for 1 mm from the end of the primary spongiosa (X-ray energy settings of 55 kVp and 109 μA). Cortical bone in the diaphysis of the tibia proximal and adjacent to the tibiofibular joint was analyzed using 40 serial cross-sectional slices. Quantitative analysis of trabecular bone of the proximal tibial metaphysis included: bone volume/total volume (BV/TV, %); trabecular number (TbN, 1/mm), thickness (TbTh, mm), separation (TbSp, mm); structural mineral index (SMI); and connective density (ConnD, 1/mm^3). Image analysis and 3D reconstructions, including midsagittal cross-sections (as determined by scanning), were performed using manufacturer software.

2.3. Blood and serum biomarkers.

Circulating white blood cell counts after 6 weeks of E_2 supplementation (vs. age-matched controls) were determined using a Hemavet 950DS (Drew Scientific, Miami Lakes, FL). E_2 levels in serum collected 2 or 6 weeks post pellet placement, and stored at −80°C prior to assay, were assayed by the University of Virginia Center for Research in Reproduction Ligand Assay and Analysis Core using a commercially available mouse/rat estradiol ELISA (Calbiotech, El Cajon, CA)[38]. Markers of bone formation (rat/mouse P1NP) or resorption (mouse TRAcP 5b) were assayed in fasting serum collected 2 weeks after start of E_2 supplementation (vs. age-matched controls) using commercially available ELISAs (Immunodiagnostic Systems, United Kingdom) [22,25].

2.4. Bone Histology.

Hind limbs were removed 6 weeks post-pellet placement from E_2 supplemented vs. age-matched control mice, fixed, decalcified and paraffin-embedded for histologic analyses. Midsagittal (approximate depth of 400–600 μm) 5-μm sections were stained with hematoxylin and eosin (H&E) to assess estrogenic effects on bone and bone marrow [39]. Multinucleated osteoclasts were identified by tartrate-resistant acid phosphatase (TRAP) staining [Acid Phosphatase, Leukocyte (TRAP) Kit, Sigma Aldrich, St. Louis, MO][39] and hematoxylin stained osteoblasts were identified as mononuclear cuboidal cells lining bone surfaces [40,41]. Osteoclasts or osteoblasts lining trabecular bone surfaces were identified in a blinded fashion 0.25 mm below the proximal tibial growth plate and reported as cell number per mm of bone surface (BS) [40] or per tissue area (mm^2). Immunohistochemical staining using a polyclonal antibody recognizing human and murine Special AT-Rich Sequence-Binding Protein 2 (SATB2; #bs-11949R, Bioss Antibodies, Woburn, MA), a nuclear protein in osteoblast lineage cells used clinically to identify osteosarcomas [42,43], was performed using previously described methods and controls [39,44] and antigen unmasking with citrate buffer (pH 6.0; Thermo Fisher Scientific, Waltham, MA) at 60°C overnight.

2.5. Statistical Analysis.

Data are reported as mean ± SEM. Statistical differences were determined using one- or two-way analyses of variance (ANOVA) with Tukey, Bonferonni, or Newman-Keuls post-hoc testing or test for linear trend (for AUC), as indicated (Prism 6.0 software, Graphpad, San Diego, CA). Statistical significance was defined as p 0.05 with all p-values two-sided.

3. Results

3.1. Effects of E_2 on bone acquisition vary with skeletal age, but were not dose-dependent

In naïve control mice, tibial bone mineral content (BMC, Fig 1A) and bone area (BA, Fig 1B) increased steadily from 4 weeks of age, achieving maximal levels by 15 weeks (53% increase, p 0.0001) and 10 weeks of age (23% increase, p 0.0001), respectively. When E_2 supplementation was begun in 4-week-old female nude mice, an age frequently used for ER- and ER+ breast cancer bone metastasis models [3,17,24,30,45–47], BMC was further stimulated by all doses tested, increasing by 32% (relative to age matched controls after 6 weeks of supplementation) in a fashion that was not dose dependent (Fig 1A). In contrast, E_2 suppressed the normal increase in BA in these developing mice, again in a fashion that was not dose-dependent, resulting in BA 10% lower than age-matched controls (Fig 1B). These dichotomous effects of E_2 supplementation on BMC and BA in 4-week-old mice resulted in an areal bone mineral density (BMD = BMC/BA) 45% higher than age-matched controls after 6 weeks of supplementation (Fig 1B, **inset**). When E_2 supplementation was instead begun at 15 weeks of age, after maximal BMD and BA had already been achieved (referred to as skeletally mature mice), E_2 induced an increase in BMC after 6 weeks of supplementation that was similar in magnitude to young mice (28% increase relative to age matched controls, Fig 1A). However, BA was unchanged (Fig 1B). Thus, the E_2-induced increase in BMD in skeletally mature mice (26% vs age-matched controls) was less than in

younger mice (Fig 1B **inset**), as was also evident from histologic examination of midsagittal tibial sections of young vs skeletally mature E_2-supplemented mice (Fig 2).

3.2. Effects of E_2 on bone microarchitecture vary with skeletal age, but were not dose-dependent

Increases in diaphyseal cortical bone and metaphyseal trabecular bone were evident in reconstructed microCT images of young or skeletally mature mice tibiae 6 weeks following the start of E_2 (0.72 mg) treatment, as compared to age-matched (10 or 21 week) controls (Fig 3A). Trabecular BV/TV (Fig 3B, first panel) increased in E_2-treated mice and achieved values in young mice that exceeded those in skeletally mature mice (91% vs 59%, respectively, for 0.72 mg E_2 dose, p 0.0001). TbN increased similarly in young and skeletally mature mice in response to E_2, while TbTh only increased in young E_2-treated mice (Fig 3B), with neither change in young mice being statistically E_2 dose-dependent. Interestingly, ConnD (Fig 3B), which does not correlate with absolute density [48], only increased significantly in skeletally mature mice in response to E_2 supplementation. SMI (Fig 3B), a measure of bone microarchitecture that typically approaches 0 for plates vs 3 for rods, with concave surfaces yielding negative values [49,50], averaged 1.7±0.10 in controls and yielded negative values for mice supplemented with E_2 at 4 weeks of age, consistent with their extremely high bone volume fraction [51]. In contrast, E_2 supplementation in skeletally mature mice, which resulted in smaller increases in BV/TV, did not significantly alter SMI. TbSp (Fig 3B), the only variable that differed between 10 vs 21 week control mice, decreased significantly and to similar levels in mice of both ages in response to E_2 treatment. This measure of hematopoietic marrow thickness was only 14% or 18% of age-matched control values in young vs. skeletally mature E_2-treated mice, respectively. Given this marked reduction in marrow cavity thickness in trabecular metaphyseal bone and similarly striking qualitative decreases in diaphyseal bone marrow space (Fig 3A), circulating white blood cell levels were examined 6 weeks after supplementation of young mice with low (0.05 mg) or high (0.72 mg) E_2 (Fig 4). Total white blood cell and lymphocyte counts were significantly decreased in young mice treated with the highest (0.72 mg) E_2 doses (vs age-matched controls), with no significant difference between the highest and lowest (0.05 mg) doses. Smaller declines in circulating neutrophil numbers (−21% vs −53% for lymphocytes) were not statistically significant. There was no evidence of splenomegaly, an indication of extramedullary hematopoiesis [52], as measured by spleen weight 2 weeks post-pellet in young or skeletally mature mice, as compared to controls (n=5/group; data not shown).

3.3. Effects of E_2 on bone turnover vary with skeletal age

Serum biomarkers of bone formation (procollagen type 1 N-terminal propeptide, P1NP) and resorption (type-5 tartrate-resistant acid phosphatase, TRAcP) were assessed at a time when E_2-induced changes in BMC and/or BA had not yet reached a maximum (2 weeks post-pellet) in young and mature mice supplemented with the highest (0.72 mg) dose of E_2 (n=5/group) (Fig 5A). As reflective of their developing skeletons, young (6 week old) control mice had significantly higher levels of P1NP than did mature control mice (Fig 5A, left panel, p 0.01), with no differences in TRAcP (Fig 5A, right panel). E_2 treatment significantly increased both formation and resorption markers in young mice (38% and 48%

increase for P1NP and TRAcP, respectively, p 0.05). By contrast, in mature animals, E_2 treatment did not alter formation markers (Fig 5A, left panel), while resorption markers declined by 52%, although this difference did not reach statistical significance (Fig 5A, right panel). Notably, both P1NP and TRAcP were 3-fold lower in skeletally mature (vs young) E_2-treated mice (Fig 5A). Histomorphometric measurements of osteoblast and osteoclast numbers were also analyzed in tibiae 2 weeks post-pellet. Consistent with increased P1NP values in E_2-treated young mice, osteoblast numbers per mm of bone surface were increased, though the trend did not reach statistical significance (Fig 5B, left panel). However, because the amount of trabecular bone surface (BS) per tissue area also significantly increased 2 weeks post-pellet in E_2-treated young and mature mice (67.5% and 123.4% increase vs age-matched controls, respectively [p 0.01]), cell counts per tissue area, which can influence circulating biomarker levels, were also ascertained (Fig 5C). In young mice treated with E_2, both osteoblast and osteoclast cell numbers per tissue area were significantly increased (Fig 5C) in parallel with increases in circulating levels of P1NP and TRAcP (Fig 5A). In mature mice, neither osteoblast nor osteoclast cell number per bone surface were altered by E2 treatment (Fig 5B), while cell counts per tissue area tended to increase, a trend that did not achieve statistical significance (Fig 5C).

3.4. Circulating E_2 levels in E_2-pelleted mice were not sustained

Circulating E_2 levels in naïve control athymic female mice (4.5±0.9 pg/ml; Fig 6) were lower than those reported for post-menopausal women (10 – 20 pg/ml) [53]. Dose-dependent increases in serum E_2 levels were documented 2 weeks post-placement of 60-day release pellets, being increased 13-fold in young mice supplementation with the lowest dose pellet (0.05 mg) or 299-fold in mice supplemented with the highest (0.72 mg) dose E_2 pellets (Fig 6, 2 weeks). However, these levels were not sustained (Fig 6, 6 weeks). By day 42 post-E_2 pellet placement, elevated circulating E_2 levels, while considerably reduced, only persisted in mice supplemented with the three highest dose 60-day release pellets (0.18, 0.36, and 0.72 mg E_2), and ranged from 4.0 – 79.1 pg/ml. Evidence of urinary retention, a well-characterized side effect of supraphysiologic levels of E_2 in nude mouse models [54,55], was observed in a subset of young animals (37.5%), and none in mature animals, following a median time of 5 weeks of supplementation with the three highest E_2 doses (0.18, 0.36, and 0.72 mg; n=8/group), though effects were not severe enough for early termination of experiments. Uterine weights (a frequent bioassay for estrogenic effects [56]) measured at 2 and 6 weeks post-pellet did not change with E_2 treatment in these ovary-intact mice as compared to controls, irrespective of age or E_2 dose (n=4–5/group; data not shown).

3.5. E_2 induced osteolytic osteosarcomas

Following E_2 pellet placement, osteolytic lesions were evident on radiographic imaging of proximal tibiae (Fig 7A) in a subset of mice. Histologically, tumors associated with radiographic lesions (Fig 7B) stained positive for SATB2, a nuclear protein in osteoblast lineage cells used clinically to identify osteosarcomas [42,43] (Fig 7C, brown nuclear staining; with corresponding H&E in Fig 7D); appeared mesenchymal (Fig 7D); and contained TRAP+ multinucleated osteoclasts in proximity to bone (Fig 7E; red staining; with corresponding H&E in Fig 7F).

These osteolytic osteosarcomas appeared in tibiae of both E_2-pelleted young and mature mice as early as 3 weeks post E_2 pellet (time-course of young mice pelleted with 0.72 mg E_2 shown in Fig 7G **inset**). Six weeks post-pellet, visible osteolytic lesions were detected in 38 – 88% of tibiae in young mice treated with 0.10 – 0.72 mg E_2, and ranged in size from 0.18 – 3.49 mm^2, with no detectable lesions in mice pelleted with the lowest E_2 dose (Fig 7G, n=4–8/group). An E_2 dose-dependent trend in lesion size was not statistically different. Although the incidence of lesion formation was lower in tibiae of E_2-pelleted mature mice compared to young mice with the same E_2 dose (33% vs 63%, respectively)(Fig 7G, white bars), lesion areas were similar (1.49 vs 1.19 mm^2, respectively)(Fig 7G, black bars). Sites other than hind limbs were not systematically examined for tumor formation.

4. Discussion

Dose or age dependent effects of 17β-estradiol (E_2) on bone have not, to our knowledge, previously been reported for female nude mice, which are frequently used to study human breast cancer xenografts, including bone metastatic tumors [10–14,17–30]. All E_2 doses tested here (0.05 – 0.72 mg) yielded the same effects on bone acquisition in young mice (as measured by BMC, BA, BMD, BV/TV, and trabecular microarchitecture). BMC was increased to a similar extent in young and in skeletally mature mice, though gains in BMD (and BV/TV in trabecular compartments) were higher in young mice, where suppression of normal increases in BA in these growing mice was one additional impact of E_2 treatment. Although young and mature mice both gained BMD with E_2-treatment, mechanisms appeared to differ. Already high levels of bone turnover increased further in young mice treated with E_2, where significant increases P1NP and osteoblast numbers were consistent with increased formation driving bone changes, while in skeletally mature mice, E_2 effects appeared more nuanced. Bone formation markers remained low in E_2-treated mature (vs young) mice, while TRAcP levels tended to decreased, suggesting decreased resorption was contributing to bone increases in these mice. Running counter to this evidence, osteoclast numbers in tibiae were somewhat increased. While discordance between histomorphometric cell counts and circulating bone turnover biomarkers are not uncommon in mouse models, including ovariectomized nude mice, it is also possible that among those osteoclasts noted in E2-treated bone were non-functioning cells induced by supraphysiologic levels of E_2, as has been reported by Gruber et al [20,58–62].

Of note, the range of E_2 doses tested here (0.05 – 0.72 mg) encompasses the low end of pellet doses specified by the manufacturer for use in immunodeficient mice (0.18 – 1.7 mg). Most importantly, because E_2 doses of 0.05 – 1.7 mg are required to sustain orthotopic ER+ breast cancer tumor growth [10,12–14], the findings presented here suggests that bone microenvironment effects of E_2 may be unavoidable in human xenograft models of ER+ breast cancer.

This marked increase in bone volume resulted in a concomitant decrease in marrow space that was associated with a significant decrease in circulating lymphocytes, which, unlike humans, are the predominant white blood cell type in the circulation of mice [63]. Because inhibitory effects of E_2 on the differentiation and proliferation of B lymphocytes are well described [64–66], the relative potential contributions of E_2-induced loss of marrow space

vs. possible direct effects of E_2 on B lymphocytes to circulating lymphocyte reductions in these T-cell deficient mice cannot be ascertained here. However, decreases in marrow space and circulating lymphocytes were documented at a time when E_2 release was minimal and uterine sizes were unchanged (contrary to reported increases in E_2-treated non-OVX mice of other strains [52,53,55]), suggesting a possible contribution of the marked reduction in marrow space (up to 86% loss in trabecular metaphyses) to decreases in circulating lymphocytes.

The range of 60-day release E_2 pellet doses tested here succeeded in achieving supraphysiologic levels of E_2 at the 2-week time-point that were comparable to, or exceeded, values present in premenopausal women [53]. However, by 42 days (week 6), E_2 levels had plummeted and were only notably increased in mice treated with the three highest pellet doses (0.18, 0.36, 0.72 mg E_2). This lack of sustained E_2 release from these commonly used commercial pellets is well documented in the literature [56,67] and could influence the *in vivo* growth of E_2 dependent tumors.

One unanticipated finding in this study was the occurrence and radiographic detection of osteolytic osteosarcomas in young and skeletally mature mice treated with all but the lowest dose of E_2. These E_2-dependent osteosarcomas were located in the proximal tibiae, which is also a common location for osteosarcomas in humans [68,69]. E_2-induced increases in bone formation may be driving the progression of these osteoblastic mesenchymal tumors in E_2 pelleted female nude mice, consistent with previous reports of osteosarcoma formation in immunocompetent mice treated orally with E_2 from birth [70] or rats treated with recombinant human parathyroid hormone (rhPTH; Teriparatide), another anabolic hormone [71,72]. From an experimental standpoint, because osteolytic bone metastases frequently occur in the proximal tibia in murine models of human breast cancer [3], secondary methods —other than radiographic imaging—may thus be needed to validate the presence of osteolytic human breast cancer bone metastases in E_2-treated nude mice, such as bioluminescence imaging of luciferase-expressing breast cancer cell lines, or immunohistochemical identification of human metastatic tumors with human and/or epithelial cell markers.

One limitation of these studies is the use of a single type of immunodeficient mice (nude) and a single nude mouse strain (outbred *Foxn1^nu*, Envigo). However, significant increases in bone acquisition have also been noted by other investigators in inbred nude mice (BALBc [22]) or outbred nude mice from other vendors in response to single doses of the same commercial E_2 pellets used here [28], suggesting that significant changes in the bone microenvironment may occur in all *Foxn1^nu* athymic nude mouse strains used for human xenograft models of E_2-dependent tumors.

In conclusion, doses of E_2 that have been reported to support the growth of orthotopic and bone metastatic ER+ breast cancers cause significant changes to the bone microenvironment that must be accounted for when assessing human xenograft bone metastases models, including the potential development of osteolytic murine osteosarcomas.

Acknowledgments:

References

[1]. Redig AJ, McAllister SS, Breast cancer as a systemic disease: a view of metastasis., J. Intern. Med 274 (2013) 113–26. doi:10.1111/joim.12084. [PubMed: 23844915]

[2]. Holen I, Speirs V, Morrissey B, Blyth K, In vivo models in breast cancer research: progress, challenges and future directions, Dis. Model. Mech 10 (2017) 359–371. doi:10.1242/dmm.028274. [PubMed: 28381598]

[3]. Wright LE, Ottewell PD, Rucci N, Peyruchaud O, Pagnotti GM, Chiechi A, Buijs JT, Sterling JA, Murine models of breast cancer bone metastasis., Bonekey Rep. 5 (2016) 804. doi:10.1038/bonekey.2016.31. [PubMed: 27867497]

[4]. Özdemir BC, Sflomos G, Brisken C, The challenges of modeling hormone receptor-positive breast cancer in mice, Endocr. Relat. Cancer 25 (2018) R319–R330. doi:10.1530/ERC-18-0063. [PubMed: 29563191]

[5]. Morgan RA, Human Tumor Xenografts: The Good, the Bad, and the Ugly, Mol. Ther 20 (2012) 882. doi:10.1038/MT.2012.73. [PubMed: 22549804]

[6]. Nilsson ME, Vandenput L, Tivesten Å, Norlén A-K, Lagerquist MK, Windahl SH, Börjesson AE, Farman HH, Poutanen M, Benrick A, Maliqueo M, Stener-Victorin E, Ryberg H, Ohlsson C, Measurement of a Comprehensive Sex Steroid Profile in Rodent Serum by High-Sensitive Gas Chromatography-Tandem Mass Spectrometry, Endocrinology. 156 (2015) 2492–2502. doi:10.1210/en.2014-1890. [PubMed: 25856427]

[7]. Zhao H, Zhou L, Shangguan AJ, Bulun SE, Aromatase expression and regulation in breast and endometrial cancer., J. Mol. Endocrinol 57 (2016) R19–33. doi:10.1530/JME-15-0310. [PubMed: 27067638]

[8]. Sjögren K, Lagerquist M, Moverare-Skrtic S, Andersson N, Windahl SH, Swanson C, Mohan S, Poutanen M, Ohlsson C, Elevated Aromatase Expression in Osteoblasts Leads to Increased Bone Mass Without Systemic Adverse Effects, J. Bone Miner. Res 24 (2009) 1263–1270. doi:10.1359/jbmr.090208. [PubMed: 19257817]

[9]. Köpf-Maier P, Mboneko VF, Anomalies in the hormonal status of athymic nude mice, J. Cancer Res. Clin. Oncol 116 (1990) 229–231. doi:10.1007/BF01612895. [PubMed: 2370246]

[10]. Jordan VC, Gottardis MM, Robinson SP, Friedl A, Immune-deficient animals to study "hormone-dependent" breast and endometrial cancer., J. Steroid Biochem 34 (1989) 169–76. [PubMed: 2626014]

[11]. Noone AM CK, Howlader N, Krapcho M, Miller D, Brest A, Yu M, Ruhl J, Tatalovich Z, Mariotto A, Lewis DR, Chen HS, Feuer EJ, SEER Cancer Statistics Review, 1975–2015, National Cancer Institute., SEER Cancer Stat. Rev. 1975–2015, Natl. Cancer Institute (2018). https://seer.cancer.gov/csr/1975_2015/ (accessed April 12, 2018).

[12]. Osborne CK, Hobbs K, Clark GM, Effect of estrogens and antiestrogens on growth of human breast cancer cells in athymic nude mice., Cancer Res. 45 (1985) 584–90. [PubMed: 3967234]

[13]. Shafie SM, Liotta LA, Formation of metastasis by human breast carcinoma cells (MCF-7) in nude mice., Cancer Lett. 11 (1980) 81–7. [PubMed: 6450636]

[14]. Gottardis MM, Robinson SP, Jordan VC, Estradiol-stimulated growth of MCF-7 tumors implanted in athymic mice: a model to study the tumoristatic action of tamoxifen., J. Steroid Biochem 30 (1988) 311–4. [PubMed: 3386259]

[15]. Soni A, Ren Z, Hameed O, Chanda D, Morgan CJ, Siegal GP, Wei S, Breast cancer subtypes predispose the site of distant metastases., Am. J. Clin. Pathol 143 (2015) 471–8. doi:10.1309/AJCPYO5FSV3UPEXS. [PubMed: 25779997]

[16]. Han HH, Lee SH, Kim BG, Lee JH, Kang S, Cho NH, Estrogen Receptor Status Predicts Late-Onset Skeletal Recurrence in Breast Cancer Patients., Medicine (Baltimore). 95 (2016) e2909. doi:10.1097/MD.0000000000002909. [PubMed: 26937933]

[17]. Winding B, Misander H, Høegh-Andersen P, Brünner N, Foged NT, Estradiol enhances osteolytic lesions in mice inoculated with human estrogen receptor-negative MDA-231 breast cancer cells in vivo., Breast Cancer Res. Treat 78 (2003) 205–16. [PubMed: 12725420]

[18]. Cohen DJ, Patel V, Verma A, Schwartz Z, Effect of 17β-estradiol on estrogen receptor negative breast cancer cells in an osteolytic mouse model, Steroids. 142 (2019) 28–33. doi:10.1016/J.STEROIDS.2017.10.010. [PubMed: 29133279]

[19]. Ottewell PD, Wang N, Brown HK, Fowles CA, Croucher PI, Eaton CL, Holen I, OPG-Fc inhibits ovariectomy-induced growth of disseminated breast cancer cells in bone., Int. J. Cancer 137 (2015) 968–77. doi:10.1002/ijc.29439. [PubMed: 25603921]

[20]. Wright LE, Harhash AA, Kozlow WM, Waning DL, Regan JN, She Y, Hallberg B, Murthy S, Niewolna M, Marks AR, Mohammad KS, Guise TA, Aromatase inhibitor-induced bone loss increases the progression of estrogen receptor-negative breast cancer in bone and exacerbates muscle weakness in vivo, Oncotarget. 8 (2017) 8406–8419. doi:10.18632/oncotarget.14139. [PubMed: 28039445]

[21]. Rabbani SA, Khalili P, Arakelian A, Pizzi H, Chen G, Goltzman D, Regulation of Parathyroid Hormone-Related Peptide by Estradiol: Effect on Tumor Growth and Metastasis in Vitro and in Vivo, Endocrinology. 146 (2005) 2885–2894. doi:10.1210/en.2005-0062. [PubMed: 15831570]

[22]. Ottewell PD, Wang N, Brown HK, Reeves KJ, Fowles C. a., Croucher PI, Eaton CL, Holen I, Zoledronic Acid Has Differential Antitumor Activity in the Pre- and Postmenopausal Bone Microenvironment In Vivo, Clin. Cancer Res 20 (2014) 2922–2932. doi:10.1158/1078-0432.CCR-13-1246. [PubMed: 24687923]

[23]. Ogba N, Manning NG, Bliesner BS, Ambler S, Haughian JM, Pinto MP, Jedlicka P, Joensuu K, Heikkilä P, Horwitz KB, Luminal breast cancer metastases and tumor arousal from dormancy are promoted by direct actions of estradiol and progesterone on the malignant cells, Breast Cancer Res. 16 (2014) 489. doi:10.1186/s13058-014-0489-4. [PubMed: 25475897]

[24]. Canon J, Bryant R, Roudier M, Branstetter DG, Dougall WC, RANKL inhibition combined with tamoxifen treatment increases anti-tumor efficacy and prevents tumor-induced bone destruction in an estrogen receptor-positive breast cancer bone metastasis model., Breast Cancer Res. Treat 135 (2012) 771–80. doi:10.1007/s10549-012-2222-2. [PubMed: 22926264]

[25]. Holen I, Walker M, Nutter F, Fowles A, Evans CA, Eaton CL, Ottewell PD, Oestrogen receptor positive breast cancer metastasis to bone: inhibition by targeting the bone microenvironment in vivo., Clin. Exp. Metastasis 33 (2015) 211–224. doi:10.1007/s10585-015-9770-x. [PubMed: 26585891]

[26]. Ganapathy V, Banach-Petrosky W, Xie W, Kareddula A, Nienhuis H, Miles G, Reiss M, Luminal breast cancer metastasis is dependent on estrogen signaling., Clin. Exp. Metastasis 29 (2012) 493–509. doi:10.1007/s10585-012-9466-4. [PubMed: 22427027]

[27]. Johnson RW, Finger EC, Olcina MM, Vilalta M, Aguilera T, Miao Y, Merkel AR, Johnson JR, Sterling JA, Wu JY, Giaccia AJ, Induction of LIFR confers a dormancy phenotype in breast cancer cells disseminated to the bone marrow, Nat. Cell Biol 18 (2016) 1078–1089. doi:10.1038/ncb3408. [PubMed: 27642788]

[28]. Sowder ME, Johnson RW, Enrichment and detection of bone disseminated tumor cells in models of low tumor burden, Sci. Rep 8 (2018) 14299. doi:10.1038/s41598-018-32653-2. [PubMed: 30250146]

[29]. Li Y, Zhang H, Zhao Y, Wang C, Cheng Z, Tang L, Gao Y, Liu F, Li J, Li Y, Li Y, Geng N, Rui X, Teng Y, Liu Y, Cao L, Kumar R, Jin F, Li F, A mandatory role of nuclear PAK4-LIFR axis in breast-to-bone metastasis of ERα-positive breast cancer cells, Oncogene. 38 (2019) 808–821. doi:10.1038/s41388-018-0456-0. [PubMed: 30177834]

[30]. Thomas RJ, Guise TA, Yin JJ, Elliott J, Horwood NJ, Martin TJ, Gillespie MT, Breast cancer cells interact with osteoblasts to support osteoclast formation., Endocrinology. 140 (1999) 4451–8. doi:10.1210/endo.140.10.7037. [PubMed: 10499498]

[31]. Willinghamm MD, Brodt MD, Lee KL, Stephens AL, Ye J, Silva MJ, Age-Related Changes in Bone Structure and Strength in Female and Male BALB/c Mice, Calcif. Tissue Int 86 (2010) 470–483. doi:10.1007/s00223-010-9359-y. [PubMed: 20405109]

[32]. Glatt V, Canalis E, Stadmeyer L, Bouxsein ML, Age-Related Changes in Trabecular Architecture Differ in Female and Male C57BL/6J Mice, J. Bone Miner. Res 22 (2007) 1197–1207. doi:10.1359/jbmr.070507. [PubMed: 17488199]

[33]. Modder UIL, Riggs BL, Spelsberg TC, Fraser DG, Atkinson EJ, Arnold R, Khosla S, Dose-response of estrogen on bone versus the uterus in ovariectomized mice., Eur. J. Endocrinol 151 (2004) 503–10. [PubMed: 15476452]

[34]. Urist MR, Budy AM, McLean FC, Endosteal-bone formation in estrogen-treated mice., J. Bone Joint Surg. Am 32A (1950) 143–62, illust. [PubMed: 15409259]

[35]. Turner CH, Hsieh Y-F, Müller R, Bouxsein ML, Baylink DJ, Rosen CJ, Grynpas MD, Donahue LR, Beamer WG, Genetic Regulation of Cortical and Trabecular Bone Strength and Microstructure in Inbred Strains of Mice, J. Bone Miner. Res 15 (2000) 1126–1131. doi:10.1359/jbmr.2000.15.6.1126. [PubMed: 10841181]

[36]. Bouxsein ML, Myers KS, Shultz KL, Donahue LR, Rosen CJ, Beamer WG, Ovariectomy-Induced Bone Loss Varies Among Inbred Strains of Mice, J. Bone Miner. Res 20 (2005) 1085–1092. doi:10.1359/JBMR.050307. [PubMed: 15940361]

[37]. Cenci S, Weitzmann MN, Roggia C, Namba N, Novack D, Woodring J, Pacifici R, Estrogen deficiency induces bone loss by enhancing T-cell production of TNF-alpha., J. Clin. Invest 106 (2000) 1229–37. doi:10.1172/JCI11066. [PubMed: 11086024]

[38]. Haisenleder DJ, Schoenfelder AH, Marcinko ES, Geddis LM, Marshall JC, Estimation of estradiol in mouse serum samples: evaluation of commercial estradiol immunoassays., Endocrinology. 152 (2011) 4443–7. doi:10.1210/en.2011-1501. [PubMed: 21933867]

[39]. Wright LE, Frye JB, Lukefahr AL, Timmermann BN, Mohammad KS, a Guise T, Funk JL, Curcuminoids block TGF-β signaling in human breast cancer cells and limit osteolysis in a murine model of breast cancer bone metastasis., J. Nat. Prod 76 (2013) 316–21. doi:10.1021/np300663v. [PubMed: 23145932]

[40]. Dempster DW, Compston JE, Drezner MK, Glorieux FH, Kanis JA, Malluche H, Meunier PJ, Ott SM, Recker RR, Parfitt AM, Standardized nomenclature, symbols, and units for bone histomorphometry: A 2012 update of the report of the ASBMR Histomorphometry Nomenclature Committee, J. Bone Miner. Res 28 (2013) 2–17. doi:10.1002/jbmr.1805. [PubMed: 23197339]

[41]. Streicher C, Heyny A, Andrukhova O, Haigl B, Slavic S, Schüler C, Kollmann K, Kantner I, Sexl V, Kleiter M, Hofbauer LC, Kostenuik PJ, Erben RG, Estrogen Regulates Bone Turnover by Targeting RANKL Expression in Bone Lining Cells, Sci. Rep 7 (2017) 6460. doi:10.1038/s41598-017-06614-0. [PubMed: 28744019]

[42]. Machado I, Navarro S, Picci P, Llombart-Bosch A, The utility of SATB2 immunohistochemical expression in distinguishing between osteosarcomas and their malignant bone tumor mimickers, such as Ewing sarcomas and chondrosarcomas, Pathol. - Res. Pract 212 (2016) 811–816. doi:10.1016/J.PRP.2016.06.012. [PubMed: 27465835]

[43]. Conner JR, Hornick JL, SATB2 is a novel marker of osteoblastic differentiation in bone and soft tissue tumours, Histopathology. 63 (2013) 36–49. doi:10.1111/his.12138. [PubMed: 23701429]

[44]. Braidman IP, Hainey L, Batra G, Selby PL, Saunders PTK, Hoyland JA, Localization of Estrogen Receptor β Protein Expression in Adult Human Bone, J. Bone Miner. Res 16 (2001) 214–220. doi:10.1359/jbmr.2001.16.2.214. [PubMed: 11204421]

[45]. Mbalaviele G, Dunstan CR, Sasaki A, Williams PJ, Mundy GR, Yoneda T, E-cadherin expression in human breast cancer cells suppresses the development of osteolytic bone metastases in an experimental metastasis model., Cancer Res. 56 (1996) 4063–70. [PubMed: 8752180]

[46]. Guise TA, Yin JJ, Taylor SD, Kumagai Y, Dallas M, Boyce BF, Yoneda T, Mundy GR, Evidence for a causal role of parathyroid hormone-related protein in the pathogenesis of human breast

cancer-mediated osteolysis., J. Clin. Invest 98 (1996) 1544–1549. doi:10.1172/JCI118947. [PubMed: 8833902]

[47]. Kang Y, Siegel PM, Shu W, Drobnjak M, Kakonen SM, Cordón-Cardo C, a Guise T, Massagué J, A multigenic program mediating breast cancer metastasis to bone., Cancer Cell. 3 (2003) 537–549. doi:10.1016/S1535-6108(03)00132-6. [PubMed: 12842083]

[48]. Odgaard A, Gundersen HJ, Quantification of connectivity in cancellous bone, with special emphasis on 3-D reconstructions., Bone. 14 (n.d.) 173–82. [PubMed: 8334036]

[49]. Salmon PL, Ohlsson C, Shefelbine SJ, Doube M, Structure Model Index Does Not Measure Rods and Plates in Trabecular Bone, Front. Endocrinol. (Lausanne) 6 (2015) 162. doi:10.3389/fendo.2015.00162. [PubMed: 26528241]

[50]. HILDEBRAND T, RÜEGSEGGER P, Quantification of Bone Microarchitecture with the Structure Model Index, Comput. Methods Biomech. Biomed. Engin 1 (1997) 15–23. doi:10.1080/01495739708936692. [PubMed: 11264794]

[51]. Bouxsein ML, Boyd SK, Christiansen BA, Guldberg RE, Jepsen KJ, Müller R, Guidelines for assessment of bone microstructure in rodents using micro-computed tomography., J. Bone Miner. Res 25 (2010) 1468–86. doi:10.1002/jbmr.141. [PubMed: 20533309]

[52]. Connell NT, Shurin SB, Schiffman F, The Spleen and Its Disorders, in: Hematol. Basic Princ. Pract 7th Ed., 7th ed., Elsevier, 2018: pp. 2313–2327.

[53]. Strauss JF, Barbieri RL, Yen SSC, Yen and Jaffe's reproductive endocrinology : physiology, pathophysiology, and clinical management, 8th ed., Elsevier, 2019.

[54]. Pearse G, Frith J, Randall KJ, Klinowska T, Urinary Retention and Cystitis Associated with Subcutaneous Estradiol Pellets in Female Nude Mice, Toxicol. Pathol 37 (2009) 227–234. doi:10.1177/0192623308329281. [PubMed: 19181629]

[55]. Gakhar G, Wight-Carter M, Andrews G, Olson S, Nguyen TA, Hydronephrosis and Urine Retention in Estrogen-Implanted Athymic Nude Mice, Vet. Pathol 46 (2009) 505–508. doi:10.1354/vp.08-VP-0180-N-BC. [PubMed: 19176493]

[56]. Ingberg E, Theodorsson A, Theodorsson E, Strom JO, Methods for long-term 17β-estradiol administration to mice, Gen. Comp. Endocrinol 175 (2012) 188–193. doi:10.1016/J.YGCEN.2011.11.014. [PubMed: 22137913]

[57]. Gruber HE, Puzanov IJ, Bennett M, Kumar V, Gordon B, Alterations in osteoclast morphology following long-term 17beta-estradiol administration in the mouse., BMC Cell Biol. 2 (2001) 3. doi:10.1186/1471-2121-2-3. [PubMed: 11231877]

[58]. Wang F-S, Wu R-W, Lain W-S, Tsai T-C, Chen Y-S, Sun Y-C, Ke H-J, Li J-C, Hwang J, Ko J-Y, Sclerostin vaccination mitigates estrogen deficiency induction of bone mass loss and microstructure deterioration, Bone. 112 (2018) 24–34. doi:10.1016/j.bone.2018.04.007. [PubMed: 29653294]

[59]. Panwar P, Xue L, Søe K, Srivastava K, Law S, Delaisse J-M, Brömme D, An Ectosteric Inhibitor of Cathepsin K Inhibits Bone Resorption in Ovariectomized Mice, J. Bone Miner. Res 32 (2017) 2415–2430. doi:10.1002/jbmr.3227. [PubMed: 28745432]

[60]. Hawse JR, Pitel KS, Cicek M, Philbrick KA, Gingery A, Peters KD, Syed FA, Ingle JN, Suman VJ, Iwaniec UT, Turner RT, Spelsberg TC, Subramaniam M, TGFβ Inducible Early Gene-1 Plays an Important Role in Mediating Estrogen Signaling in the Skeleton, J. Bone Miner. Res 29 (2014) 1206–1216. doi:10.1002/jbmr.2142. [PubMed: 24190163]

[61]. Ballanti P, Minisola S, Pacitti MT, Scarnecchia L, Rosso R, Mazzuoli GF, Bonucci E, Tartrate-resistant acid phosphate activity as osteoclastic marker: Sensitivity of cytochemical assessment and serum assay in comparison with standardized osteoclast histomorphometry, Osteoporos. Int 7 (1997) 39–43. doi:10.1007/BF01623458. [PubMed: 9102061]

[62]. Marcus R, Feldman D, Nelson DA, Rosen CJ, Osteoporosis, 3rd ed., Elsevier, 2008.

[63]. O'Connell KE, Mikkola AM, Stepanek AM, Vernet A, Hall CD, Sun CC, Yildirim E, Staropoli JF, Lee JT, Brown DE, Practical Murine Hematopathology: A Comparative Review and Implications for Research, Comp. Med 65 (2015) 96. [PubMed: 25926395]

[64]. Erlandsson M, Jonsson C, Lindberg M, Ohlsson C, Carlsten H, Raloxifene- and estradiol-mediated effects on uterus, bone and B lymphocytes in mice, J. Endocrinol 175 (2002) 319–327. doi:10.1677/joe.0.1750319. [PubMed: 12429030]

[65]. Erlandsson MC, Islander U, Moverare S, Ohlsson C, Carlsten H, Estrogenic agonism and antagonism of the soy isoflavone genistein in uterus, bone and lymphopoiesis in mice, APMIS. 113 (2005) 317–323. doi:10.1111/j.1600-0463.2005.apm_113502.x. [PubMed: 16011657]

[66]. Medina KL, Strasser A, Kincade PW, Estrogen influences the differentiation, proliferation, and survival of early B-lineage precursors., Blood. 95 (2000) 2059–67. [PubMed: 10706875]

[67]. Gérard C, Gallez A, Dubois C, Drion P, Delahaut P, Quertemont E, Noël A, Pequeux C, Accurate Control of 17β-Estradiol Long-Term Release Increases Reliability and Reproducibility of Preclinical Animal Studies, J. Mammary Gland Biol. Neoplasia 22 (2017) 1–11. doi:10.1007/s10911-016-9368-1. [PubMed: 27889857]

[68]. Haynes K, Tyner C, Williams PD, Repiphysis prosthesis for limb preservation in pediatric patients with bone cancer: a literature review., Orthop. Nurs 32 (2013) 81–6; quiz 87–8. doi:10.1097/NOR.0b013e3182879bbb. [PubMed: 23518749]

[69]. Chen Y, Yu X, Xu S, Xu M, Song R, Impacts of Tumor Location, Nature and Bone Destruction of Extremity Osteosarcoma on Selection of Limb Salvage Operative Procedure, Orthop. Surg 8 (2016) 139–149. doi:10.1111/os.12237. [PubMed: 27384722]

[70]. Highman B, Roth SI, Greenman DL, Osseous Changes and Osteosarcomas In Mice Continuously Fed Diets Containing Diethylstilbestrol or 17β-Estradiol, JNCI J. Natl. Cancer Inst 67 (1981) 653–662. doi:10.1093/jnci/67.3.653. [PubMed: 6944535]

[71]. Vahle JL, Long GG, Sandusky G, Westmore M, Ma YL, Sato M, Bone Neoplasms in F344 Rats Given Teriparatide [rhPTH(1–34)] Are Dependent on Duration of Treatment and Dose, Toxicol. Pathol 32 (2004) 426–438. doi:10.1080/01926230490462138. [PubMed: 15204966]

[72]. Vahle JL, Sato M, Long GG, Young JK, Francis PC, Engelhardt JA, Westmore MS, Ma YL, Nold JB, Skeletal Changes in Rats Given Daily Subcutaneous Injections of Recombinant Human Parathyroid Hormone (1–34) for 2 Years and Relevance to Human Safety, Toxicol. Pathol 30 (2002) 312–321. doi:10.1080/01926230252929882. [PubMed: 12051548]
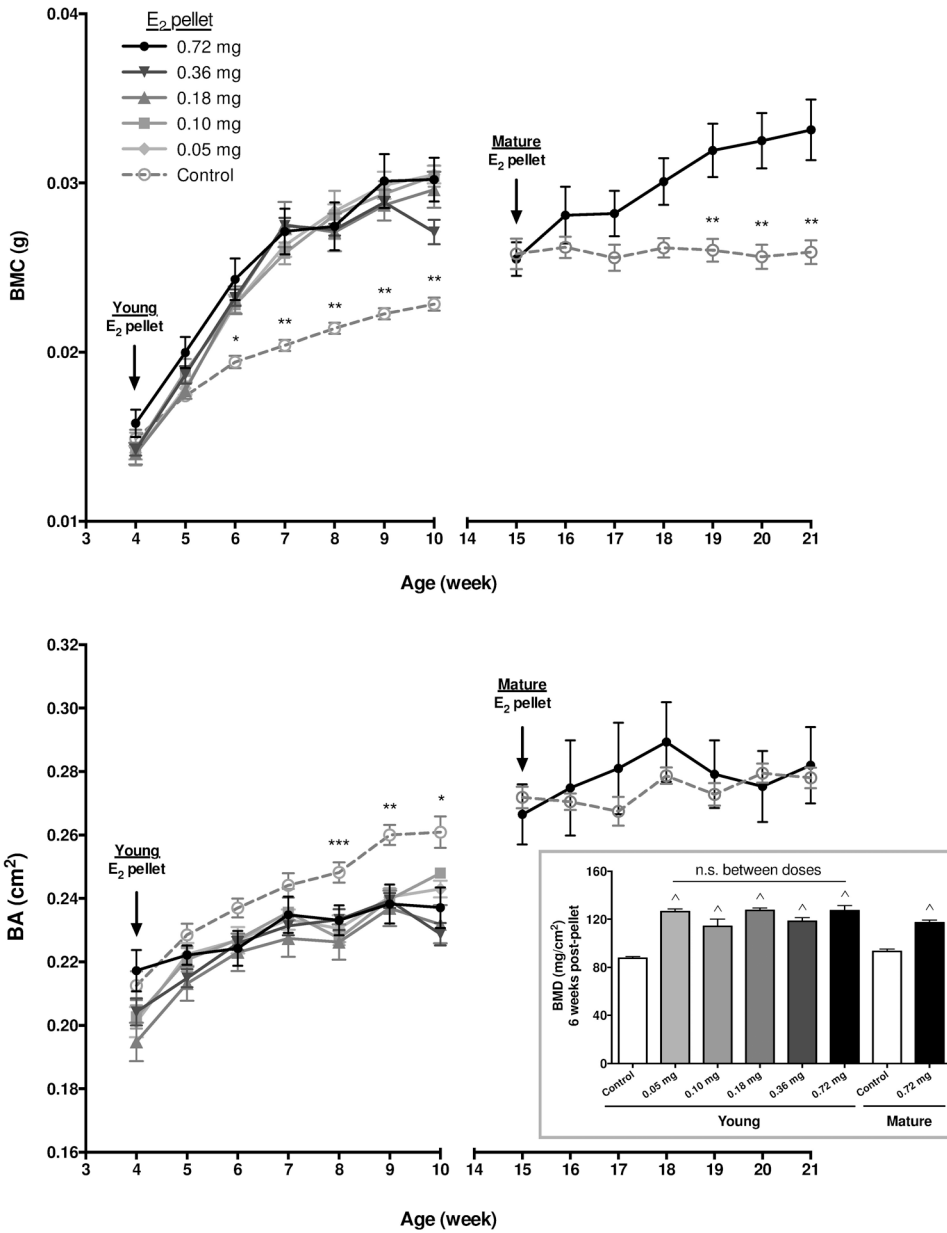
Figure 1. Effects of E$_2$ on bone as measured by DXA and histologic imaging

DXA analysis of total tibial bone mineral content (BMC; **A**) and bone area (BA; **B**) (n=6–8/ group) in mice supplemented with the indicated doses of E$_2$ (vs age-matched controls) beginning either at age of 4 weeks (young) or 15 weeks (mature). In young mice, E$_2$ increased BMC and decreased BA without any differences between E$_2$ doses at any time point as assessed by two-way ANOVA with Tukey post-test (nor was there a linear trend between doses for AUC). *p 0.05 control vs all E$_2$ doses except 0.10 mg; **p 0.05 control vs all E$_2$ doses; and *** p 0.05 control vs 0.10 mg and 0.18 mg E$_2$. For skeletally mature mice treated with high dose E$_2$, BMC increased while BA was unchanged, **p 0.01 vs age-matched control, as assessed by two-way ANOVA with Bonferroni post-test. **Inset:** Areal bone mineral density (BMD) of total tibia 6 weeks after the start of E$_2$ supplementation in

young or skeletally mature mice, ^p 0.0001 vs age-matched controls, with no statistical differences between E_2 doses (or between 10 vs. 21 week old control mice), as measured by one-way ANOVA with Tukey's post-test.
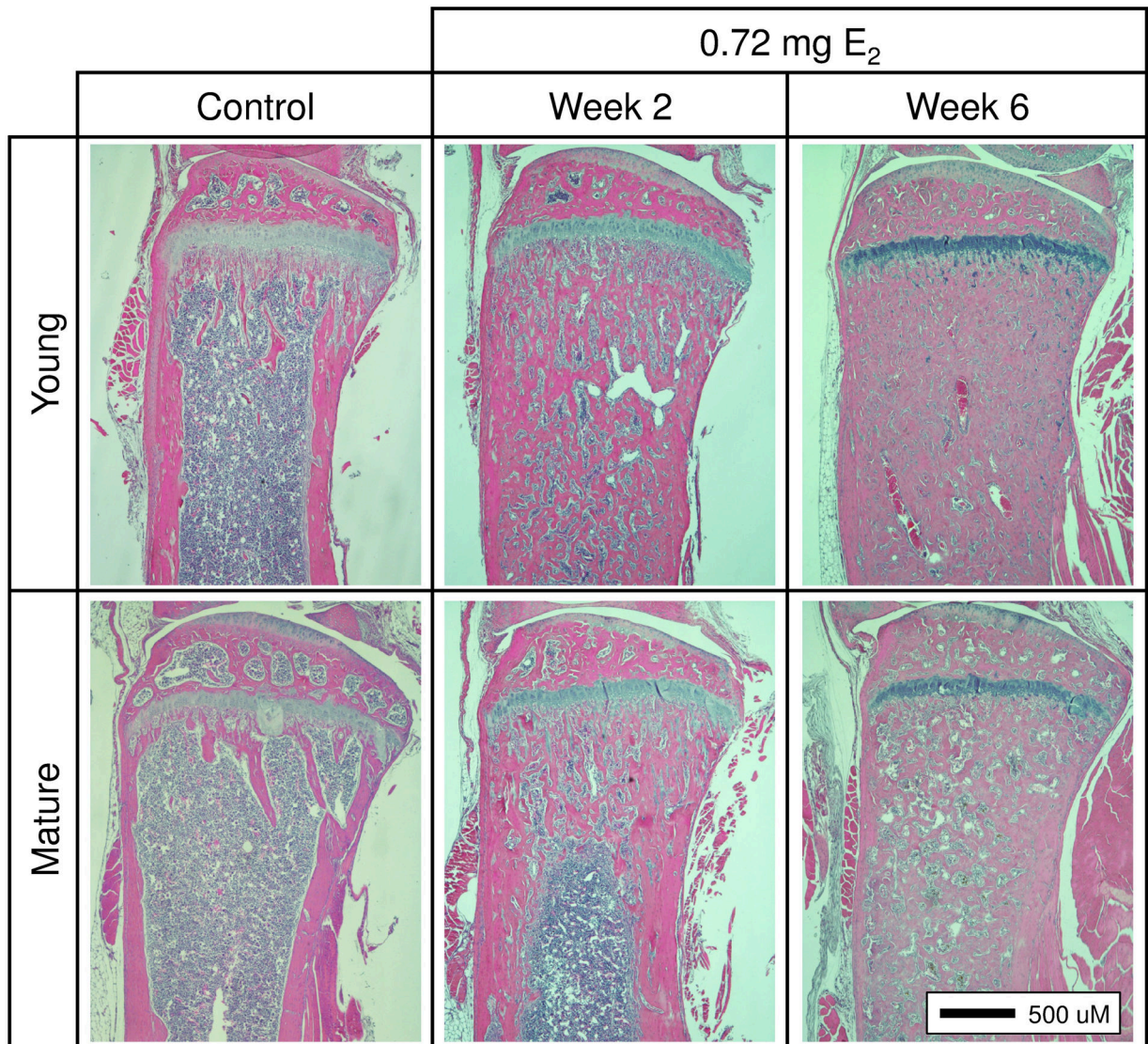
Figure 2. Effects of E$_2$ on bone histology

Histologic comparison of H&E-stained, mid-sagittal sections of proximal tibiae following 6 weeks of E$_2$ supplementation (0.72 mg) in young or skeletally mature mice (vs controls).
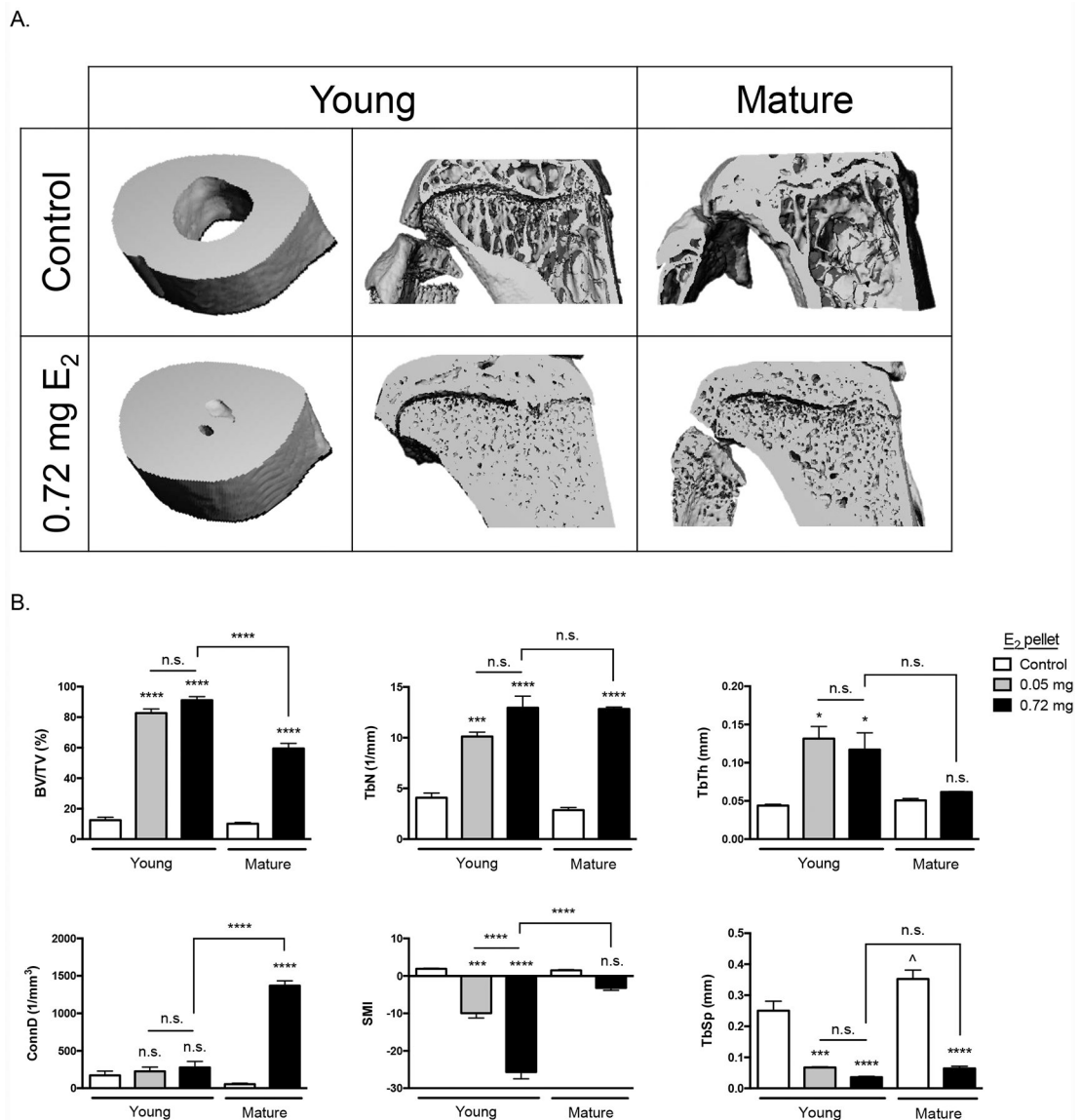
A.

B.

Figure 3. Effect of E_2 on bone microarchitecture as assessed by microCT imaging
MicroCT analysis of trabecular bone microarchitecture after 6 weeks of low (0.05 mg) or high dose (0.72 mg) E_2 supplementation beginning at 4-weeks (young) or 15-weeks (mature) of age vs aged-matched controls (10-week and 21-week-old, respectively). **A)** Representative 3D microCT images of cross-sectional tibial diaphyses and midsagittal proximal tibiae in E_2-treated young or skeletally mature mice vs age matched controls. **B)** Quantitative analysis of trabecular architecture in proximal tibial metaphyses. *p 0.05, ***p 0.001, and ****p 0.0001 (or n.s. not significant) for E_2-treated (vs. age-matched controls or group indicated by bar) by one-way ANOVA with Tukey post-test. Control mice (10 vs 21 weeks of age) only differed by TbSp values (^<p0.05). BV/TV, bone volume/total volume; TbN, trabecular number; TbTh, trabecular thickness; ConnD, connective density; SMI, structural model index; TbSp, trabecular separation.
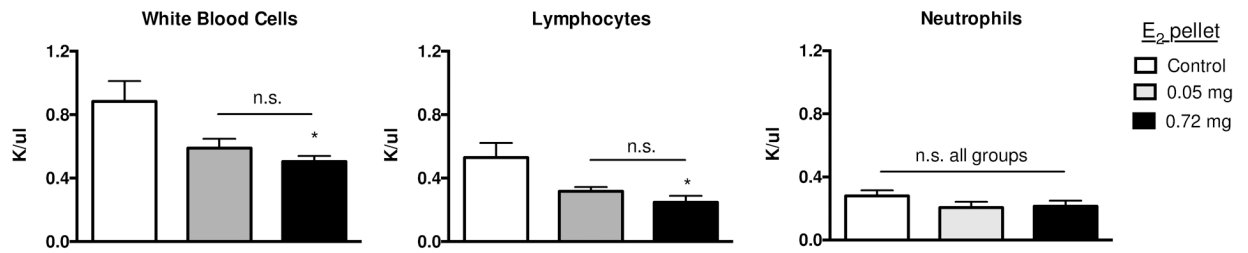
Figure 4. Effects of E$_2$ on circulating white blood cells
Circulating levels of white blood cells (left panel), lymphocytes (center panel), and neutrophils (right panel) 6 weeks post-placement of low (0.05 mg) or high (0.72 mg) E$_2$ pellets in 4-week (young) mice (vs control) (n= 4/group). *p 0.05 vs control as measured by one-way ANOVA with Tukey's post-test, with no statistical differences between E$_2$ doses (n.s.).
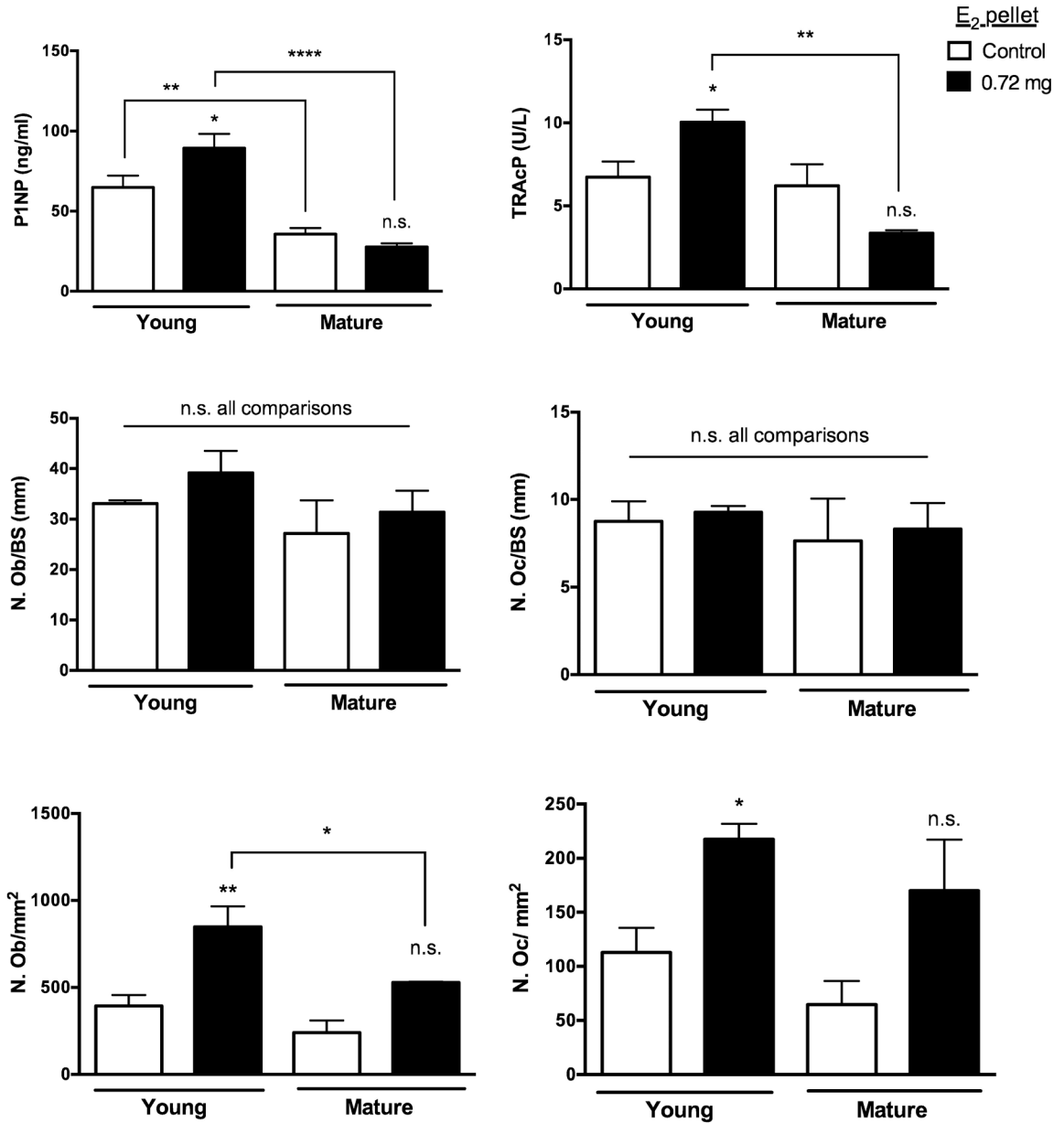
Figure 5. Effects of E$_2$ on bone turnover

A) Serum biomarkers of bone formation (P1NP; left panel) or bone resorption (TRAcP, right panel) 2 weeks after start of E$_2$ (0.72 mg) in 4-week (young) or 16-week (mature) mice vs age-matched controls (n=5/group). **B**) Osteoblast number (left panel) per bone surface (N.Ob/BS [mm]) and osteoclast number (right panel) per bone surface (N.Oc/BS [mm]) in proximal tibial metaphyses of same mice as in (A) (n=3–5/group). **C**) The number of osteoblasts (left panel) or osteoclasts (right panel) lining trabecular bone are also reported per tissue area (N./mm^2, n=3–5/group). *p ≤ 0.05 **p ≤ 0.01, or ****p ≤ 0.0001 (or n.s. not significant) for E$_2$-treated (vs. age-matched controls or group indicated by bar), as assessed by two-way ANOVA with Newman-Keuls post-test.
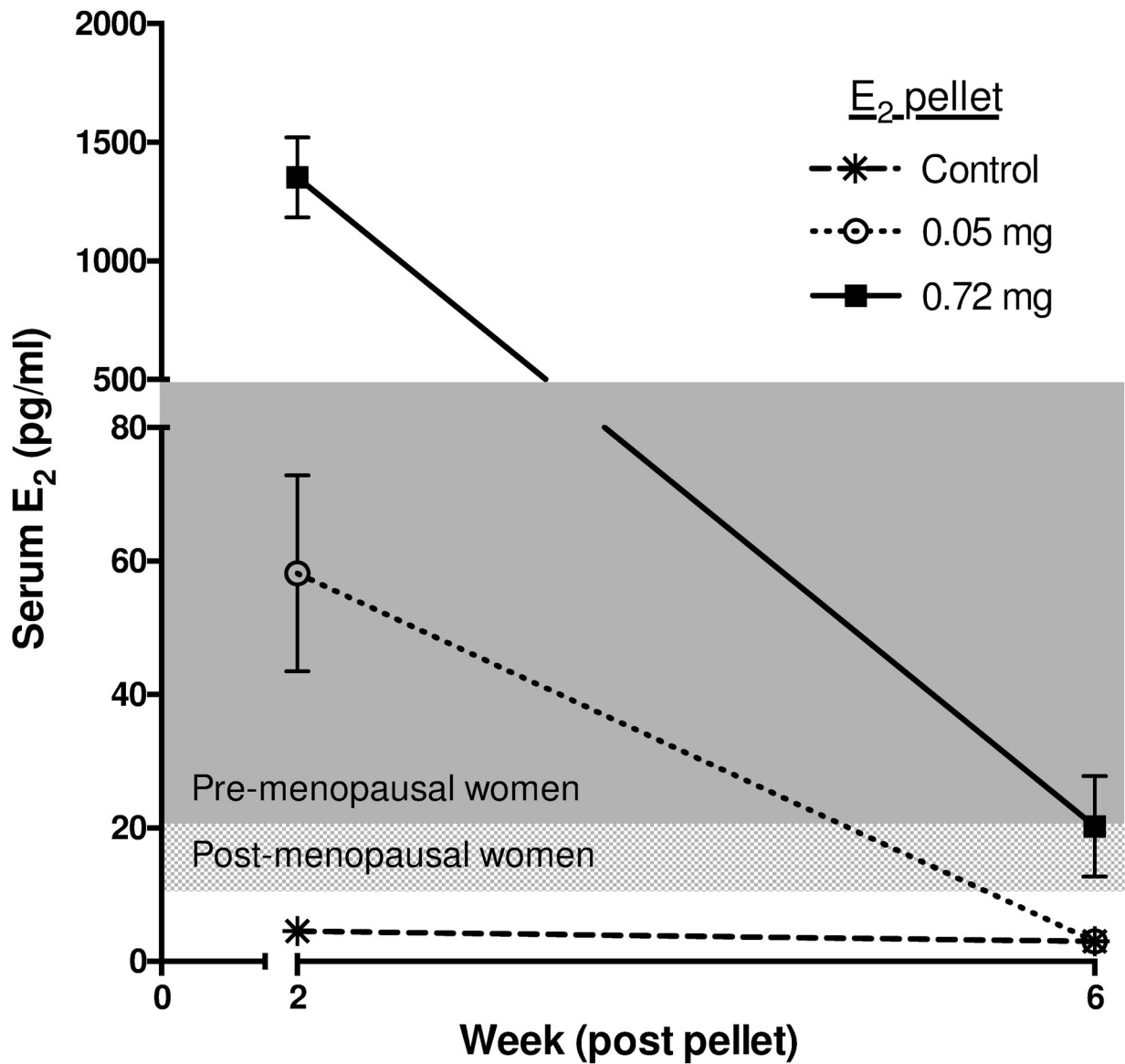
Figure 6. Circulating E$_2$ levels in E$_2$-supplemented mice

Time course of changes in serum E$_2$ levels post-placement of commercial 60-day release low (0.05 mg) or high dose (0.72 mg) E$_2$ pellets (vs. controls) in 4-week mice (n=4–5/ group). Assay limit of detection = 3.0 pg/ml. Typical E$_2$ levels in pre-menopausal (20 – 500 pg/ml) and post-menopausal (10 – 20 pg/ml) women are indicated by shading for comparison [53].
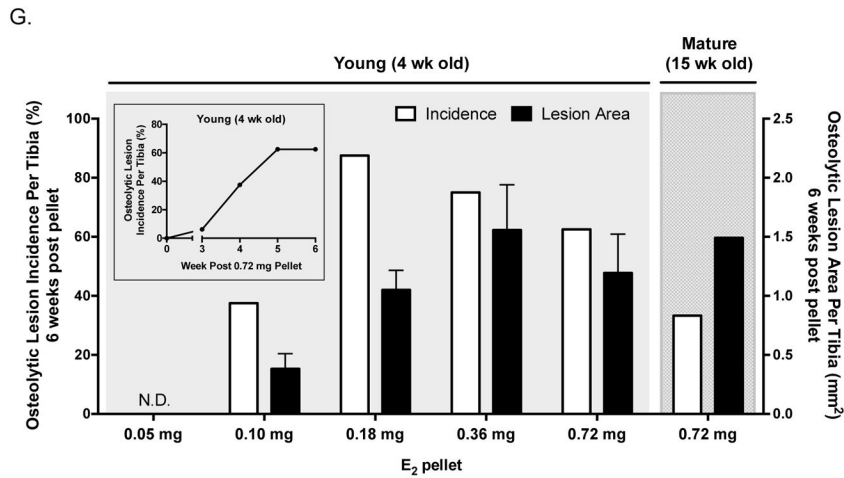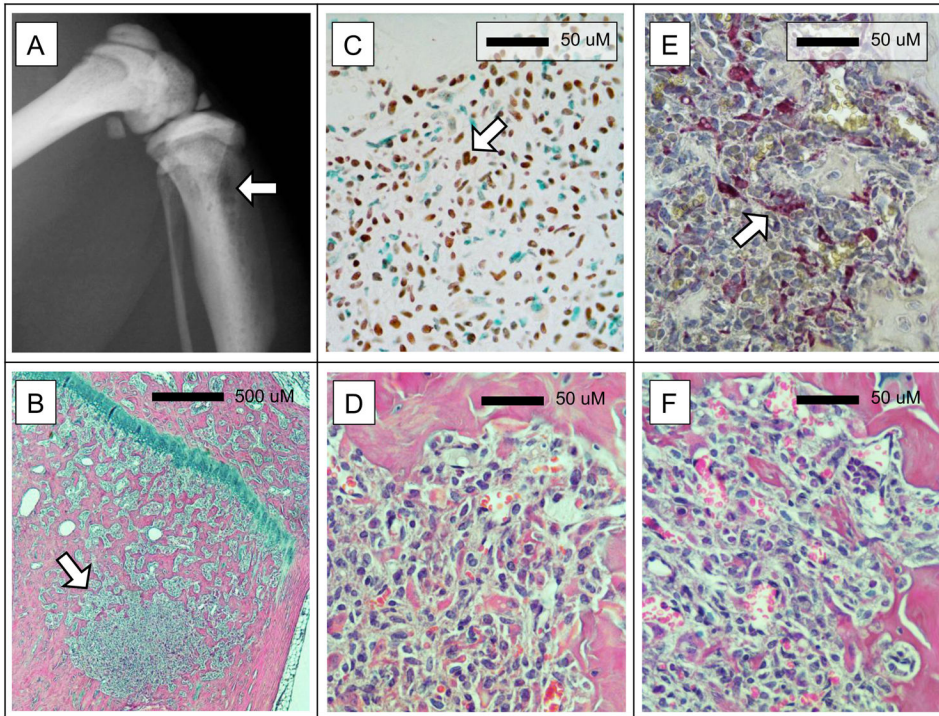
Figure 7. E$_2$ supplementation induces osteolytic osteosarcomas

Representative radiographic osteolytic lesion in proximal tibia (**A**, arrow) and corresponding midsagittal histologic section (**B**, H&E stained, arrow) 6 weeks after start of E$_2$ supplementation (0.72 mg) in 4-week old (young) mice. (**C**) Immunohistochemical detection of SATB2 (see arrow for example of mesenchymal cell with brown-stained nucleus) in representative tibial lesion (**D**, H&E) 6 weeks after start of E$_2$ supplementation (0.36 mg E$_2$) in 4-week old mice. (**E**) TRAP-positive multinucleated osteoclasts (see arrow for example of red-stained multinucleated osteoclast) in tibial lesion (**F**, H&E) 6 weeks after start of E$_2$ supplementation (0.72 mg) in 4-week old mice. (**G**) Osteosarcoma incidence (%; white bars) and lesion area size (mm^2; black bars) in tibiae of young and mature mice six weeks post-pellet with indicated E$_2$ doses, with time-course of lesion incidence in young mice pelleted

with the highest E_2 dose (0.72 mg; **inset**). In young mice that developed osteosarcomas, while power was limited due to variable incidences, lesion area was not dose dependent as determined by one-way ANOVA.